New Journal of Physics
The open–access journal for physics

Cu-based metalorganic systems: an *ab initio* study of the electronic structure

L Andrea Salguero[1], Harald O Jeschke[1,4], Badiur Rahaman[2], Tanusri Saha-Dasgupta[2], Christian Buchsbaum[3], Martin U Schmidt[3] and Roser Valentí[1]

[1] Institut für theoretische Physik, Johann Wolfgang Goethe-Universität, Max-von-Laue-Str. 1, 60438 Frankfurt/Main, Germany
[2] S N Bose National Centre for Basic Sciences, J D Block, Sector 3, Salt Lake City, Kolkata 700098, India
[3] Institut für Anorganische und Analytische Chemie, Johann Wolfgang Goethe-Universität, Max-von-Laue-Str. 7, 60438 Frankfurt/Main, Germany
E-mail: jeschke@itp.uni-frankfurt.de

New Journal of Physics **9** (2007) 26
Received 30 October 2006
Published 13 February 2007
Online at http://www.njp.org/
doi:10.1088/1367-2630/9/2/026

Abstract. Within a first principles framework, we study the electronic structure of the recently synthesized polymeric coordination compound Cu(II)-2,5-bis(pyrazol-1-yl)-1,4-dihydroxybenzene (CuCCP), which has been suggested to be a good realization of a Heisenberg spin-1/2 chain with antiferromagnetic coupling. By using a combination of classical with *ab initio* quantum mechanical methods, we design on the computer reliable modified structures of CuCCP aimed at studying effects of Cu–Cu coupling strength variations on this spin-1/2 system. For this purpose, we performed two types of modifications on CuCCP. In one case, we replaced H in the linker by (i) an electron donating group (NH_2) and (ii) an electron withdrawing group (CN), while the other modification consisted of adding H_2O and NH_3 molecules in the structure which change the local coordination of the Cu(II) ions. With the *N*th order muffin tin orbital (NMTO) downfolding method, we provide a quantitative analysis of the modified electronic structure and the nature of the Cu–Cu interaction paths in these new structures and discuss its implications for the underlying microscopic model.

[4] Author to whom any correspondence should be addressed.

PII: S1367-2630(07)36176-4

Contents

1. Introduction

Low-dimensional quantum spin systems have been a subject of intensive research in recent decades, especially in solid state theory. The discovery in recent years of low-dimensional materials has allowed a direct comparison of experimental observations with theory predictions. Out of these studies, the need for available low-dimensional materials with a certain degree of tunability has emerged since tunability has the advantage of allowing a step by step understanding of the complexity of the materials. In this paper, we will focus on the search for and study of tunable low-dimensional materials. We will restrict ourselves to a particular class of systems, namely metalorganic compounds.

Metalorganic compounds formed by transition metal centres bridged with organic ligands are being intensively discussed in the context of new molecule-based magnets and electronic materials [1, 2]. They constitute a class of tunable materials partly due to their modular nature. The modular set-up has the advantage of allowing the modification of relevant subunits chemically without changing the subsequent crystal engineering. Substitution of organic groups and ligands in these systems plays the role of doping in the search for materials with the desired magnetic interaction strengths and charge carrier concentrations.

In the present study, we pursue these ideas from a theoretical point of view. We consider a computationally feasible combination of classical with quantum mechanical *ab initio* tools [3] in order to design and analyse new metalorganic compounds. As an example, we introduce systematic changes in existing metalorganic materials in order to achieve desirable electronic or magnetic properties in the modified new structures. Such study (i) allows for a gradual understanding of the properties of these low-dimensional systems (ii) provides a guide to systematic synthesis in the laboratory.

We focus our attention on the recently synthesized coordination polymer Cu(II)-2,5-bis(pyrazol-1-yl)-1,4-dihydroxybenzene (CuCCP) [4] which, from susceptibility measurements [5], has been identified as a model system for a spin-1/2 Heisenberg chain with an antiferromagnetic exchange coupling constant of $J = 21.5\,\mathrm{K}$. The polymeric unit is shown in figure 1. This compound is a good starting point to study effects of coupling strength variation by appropriately introducing modifications on the linkers as well as changes on the Cu

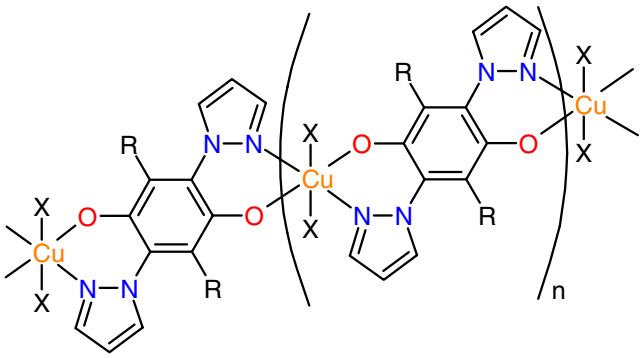

Figure 1. Polymeric unit of Cu(II)-2,5-bis(pyrazol-1-yl)-1,4-dihydroxybenzene (CuCCP) (X = ∅, R = H). We will consider the substitutions R = CN and R = NH_2 on the central benzene ring and the ligands X = H_2O and X = NH_3.

coordination. Note that the coupling strength scale for this system is small compared e.g. to inorganic Cu oxides[5] [6], where the couplings are more than one order of magnitude larger. Accordingly, in this study we will be expecting coupling strength variations in the range of one to a few tens of meV in energy.

The Cu–Cu interaction in this compound depends on the electronic nature of the linker. Its properties can be tuned smoothly and predictably by changing the substitution pattern R (see figure 1) of the central benzene ring (hydroquinone), or by introduction of additional ligands X at the Cu(II) ions. The substitution or introduction of additional ligands is expected to bring changes in the electronic properties of the compound. For example, it can change the magnitude of magnetic interactions between the Cu(II) centres in the spin chain via change in the charge density in the polymeric chain. It may change the effective inter-chain interactions, the one-dimensional nature of the original compound may thus be modified. It may even change the coordination and valence of the Cu(II) ions, which may induce changes in the transport properties along the one-dimensional chain by moving away from the Mott insulator at a half-filled Cu $3d_{x^2-y^2}$ orbital.

With the above ideas in mind, we first considered two possible H replacements in the central benzene ring: an NH_2 group, which acts as electron donating group, and a CN group, which acts as electron withdrawing group (see figure 1). Furthermore, extensive crystallization trials showed that crystallites of the Cu(II) polymer always contain lattice defects in high concentration. In many compounds, the Cu(II) ions are coordinated by six nitrogen or oxygen atoms instead of four ligands. The Cu(II) polymer is experimentally crystallized in a mixture of water and ammonia solvents, and it is likely that H_2O or NH_3 molecules are built into the crystal lattice. We have, therefore also considered the introduction of additional ligands like H_2O or NH_3 at the Cu(II) ions in our simulation study. In figure 1 and table 1, we give an account of these modified structures.

The paper is organized as follows: in section 2, we give an account of the computational methods considered in this study. In section 3, we present our results and discussion of the relaxed new crystal structures and the analysis of their electronic properties. Finally in section 4, we summarize our findings.

[5] See e.g. the case of La_2CuO_4 with J values greater than 1000 K.

Table 1. Naming convention for the substitutions and ligands on the CuCCP coordination polymer considered in this study.

Short name	R	X
CuCCP	H	–
Cu(II)–NH_2	NH_2	–
Cu(II)–CN	CN	–
Cu(II)–H_2O	H	H_2O
Cu(II)–NH_3	H	NH_3

2. Method

The methods used in this study can be primarily categorized into two classes. Firstly, a class of methods has been used for the accurate structural determination of both the parent and the modified compounds. Once the structural aspects are decided, their electronic structures are calculated and analysed with another class of methods. Note that the understanding of a complex system and design of new compounds need a combination of several different methods, each being focused to deal with one specific aspect. In the following, we give a brief description of all the methods that we have employed.

2.1. Determination of crystal structure

In the absence of diffraction data, a method much used to *a priori* predict crystal structures, is the force field technique [7]–[12]. While such calculations are computationally fast, they rely on a classical ansatz and therefore miss all possible quantum mechanical effects, which are important for the description of the electronic structure. Quantum mechanical methods, on the other side, are computationally much more demanding, and they are, in this context, typically employed for two tasks: one is the local optimization after global optimization with force field methods. This has been reported for inorganic systems like NaCl or MgF_2 [13, 14] and for simple organic compounds like glycol $C_2H_4(OH)_2$ and glycerol $C_3H_5(OH)_3$ [15]. Another is for secondary computations like the determination of molecular geometries, electrostatic charges or for the calculation of intramolecular and intermolecular potential curves [16, 17].

In the present study, we used an effective way of designing reliable crystal structures which shares the advantages of both methods, namely the fast calculations with classical force field methods and the subsequent accurate quantum mechanical description with *ab initio* methods. We first created the modified structures on the basis of crystallographic databases [18] and the crystal structures were optimized by force field methods. In the second step, the structures were relaxed by *ab initio* quantum mechanical molecular dynamics [19] within the density functional theory (DFT) formalism until the forces on the atoms were less than a given threshold to ensure structure stability. Our study differs from the previous studies mentioned in the sense that using this approach, we succeeded in treating materials with large unit cells (of the order of 100 atoms) and complicated electronic structure (transition metal complexes) with sufficient accuracy.

All force field optimizations were performed using the program package Cerius2 [20]. We modified the Dreiding 2.21 [21] force field by introducing energy terms for the case of octahedrally coordinated metal ions. For the energy minimizations we used the modified Dreiding

force field with Gasteiger [22] charges. All structural models were based on the experimentally determined crystal structure of CuCCP [4]. The crystallographic symmetry of the structure models was maintained in all relaxations. The position of the Cu ion was kept fixed during all force field and quantum mechanical optimizations. The second step of quantum mechanical relaxations were performed by Car Parrinello (CP) *ab initio* molecular dynamics (AIMD) calculations [19] based on the projector augmented wave (PAW) method [23].[6]

2.2. Electronic structure calculations

We computed the electronic structure of the relaxed structures with the full potential linearized augmented plane wave basis (FPLAPW) as implemented in the Wien2k code [24]. Calculations were performed within the generalized gradient approximation (GGA) [25]. The choice of muffin-tin radii r_{MT}, k mesh and plane-wave cutoffs $k_{\max}$ were carefully tested. We considered a k mesh of $(8 \times 6 \times 5)$ in the irreducible Brillouin zone and a $Rk_{\max} = 3.8$, which is reasonable for systems that contain hydrogen atoms.

It is well-known that local density approximation (LDA) or generalized gradient approximation (GGA) fails to describe the correct insulating ground state for a strongly correlated electron system, as is the case here. Introduction of missing correlation effects in a static mean-field like treatment as is done in the so-called LDA + U approach [26, 27], should give rise to the correct insulating state, as is supported by our calculations (not shown here). In the present paper, we are mainly interested in estimating the effective one-electron hopping interactions which are well described within LDA or GGA. In fact, the use of DFT calculations to understand the chemistry of correlated materials is a well established method [28].

Finally, in order to analyse the computed electronic structure and to extract an effective microscopic Hamiltonian, we derived quantitatively the Cu–Cu hopping integrals within the Nth order muffin tin orbital (NMTO) *downfolding* technique [29, 30] as implemented in the Stuttgart code [31].[7] The *downfolding* technique provides a useful way to derive few-orbital Hamiltonians starting from a complicated full LDA or GGA Hamiltonian by integrating out degrees of freedom which are not of interest. This procedure naturally takes into account the renormalization effect due to the integrated-out orbitals by defining energy-selected, effective orbitals which serve as Wannier-like orbitals for the few-orbital Hamiltonian in the *downfolded* representation. The method provides a first-principles way for deriving a few-band, tight-binding Hamiltonian of the form $H_{\mathrm{TB}} = \sum_{ij} t_{ij}(c_i^{\dagger} c_j + \mathrm{h.c.})$ for a complex system, where the t_{ij} define the effective hopping between the downfolded orbitals and $c_i^{\dagger}$ (c_i) are electron creation (annihilation) operators on site i. This method has proved to be extremely successful for systems such as high-T_{c} cuprates [32], double perovskites [33] or low-dimensional inorganic quantum spin systems [34]–[38].

Such estimates of the effective hopping integrals are useful in defining the underlying low-energy magnetic model. More precisely, the one-electron effective Cu–Cu hopping integral, t can be related to the Cu–Cu magnetic exchange coupling interaction J via a second-order

[6] We have performed non-spin polarized DFT calculations—in contrast to spin-polarized ones—for the structure relaxation since the energy associated with magnetism is much smaller than the cohesion energy and therefore, possible changes on the atomic positions due to the magnetic energy can be assumed to be negligible.

[7] The calculations were checked for convergence within the two choices of basis sets (FPLAPW, NMTO).

perturbative treatment within the framework a many-body Hubbard–like model. Assuming that these couplings are antiferromagnetic and neglecting ferromagnetic contributions, J can be estimated as $J_{\mathrm{AFM}} \approx 4t^2/U_{\mathrm{eff}}$ where U_{eff} is the effective onsite Coulomb repulsion on the Cu site.

3. Results

3.1. Crystal structure

Dinnebier *et al* [4] reported the synthesis, and crystal structure determination of the CuCCP system obtained by layering a solution of 2,5-bis(pyrazol-1-yl)-1,4-dihydroxybenzene in CH_2Cl_2 with a solution of $CuBr_2$ in concentrated aqueous ammonia. The system crystallizes in the triclinic space group $P\bar{1}$ with 27 atoms per unit cell. This compound tends to form independent polymeric chains consisting of deprotonated 2,5-bis(pyrazol-1-yl)-1,4-dihydroxybenzene molecules bridged by Cu(II) ions with a $3d^9$ configuration, which corresponds to a local spin-1/2. As shown in figure 2 the chain axes are oriented along the c-axis of the crystal and the copper ions are located at (1/2, 1/2, 1/2), which is a centre of symmetry of the space group $P\bar{1}$. The Cu–Cu distance along the approximate a-axis is about 5.2 Å while along the other two axes it is close to 8 Å. These Cu(II) ions are coordinated in an almost square planar fashion by two (pyrazolyl) nitrogen atoms and two oxygen atoms of the deprotonated dihydroxybenzene groups.

The crystal structure was determined from x-ray powder diffraction data; consequently the overall structure and the arrangement of the chains are reliable, but the individual atomic positions had an accuracy of only about 0.3 Å. A DFT analysis of the forces [24] between the atoms shows that the experimentally determined CuCCP structure is still very unstable with forces of the order of 100 mRyd per a_{B} or more for some atoms. We have therefore relaxed the atomic positions keeping the Cu position fixed with the AIMD method described in subsection 2.1.

The Cu(II)–NH_2 polymer and the Cu(II)–CN polymer were generated from the CuCCP polymer, by substituting the two hydrogen atoms of the benzene rings by amino (NH_2) or cyano (CN) groups, respectively (see figure 1 and table 1). The Cu(II)–H_2O (Cu(II)–NH_3) polymer was constructed from the CuCCP polymer by adding two water molecules (ammonia molecules) as additional ligands to the Cu(II) ion (see figure 1 and table 1). In the original crystal structure the chains are quite densely stacked. The introduction of the H_2O (or NH_3) molecules would either lead to unrealistically short contacts to the neighbouring chains, or to a considerable increase of the distances between the chains, resulting in an unrealistically loosely packed structure. Therefore the crystal structures of the Cu(II)–H_2O and Cu(II)–NH_3 polymers were fully optimized, including an optimization of the lattice parameters. Moreover, in order to achieve a better packing of the Cu(II) polymer chains with a favourable lattice energy, the Cu(II) chains shifted in the optimization process both sideways as well as along the chain direction with respect to each other. The resulting unit cell parameters are shown in table 2.

All the modified structures were relaxed in the second step with the AIMD method until the forces on the atoms were sufficiently small to ensure stability of the quantum mechanical calculations. In the appendix, we present the relaxed structural data of all the modified structures.

3.2. Electronic structure and effective Cu–Cu interactions

3.2.1. CuCCP. In figure 3, we present the band structure for the relaxed CuCCP where the Cu d band character is shown by bars on the right side. The band characters are given in the

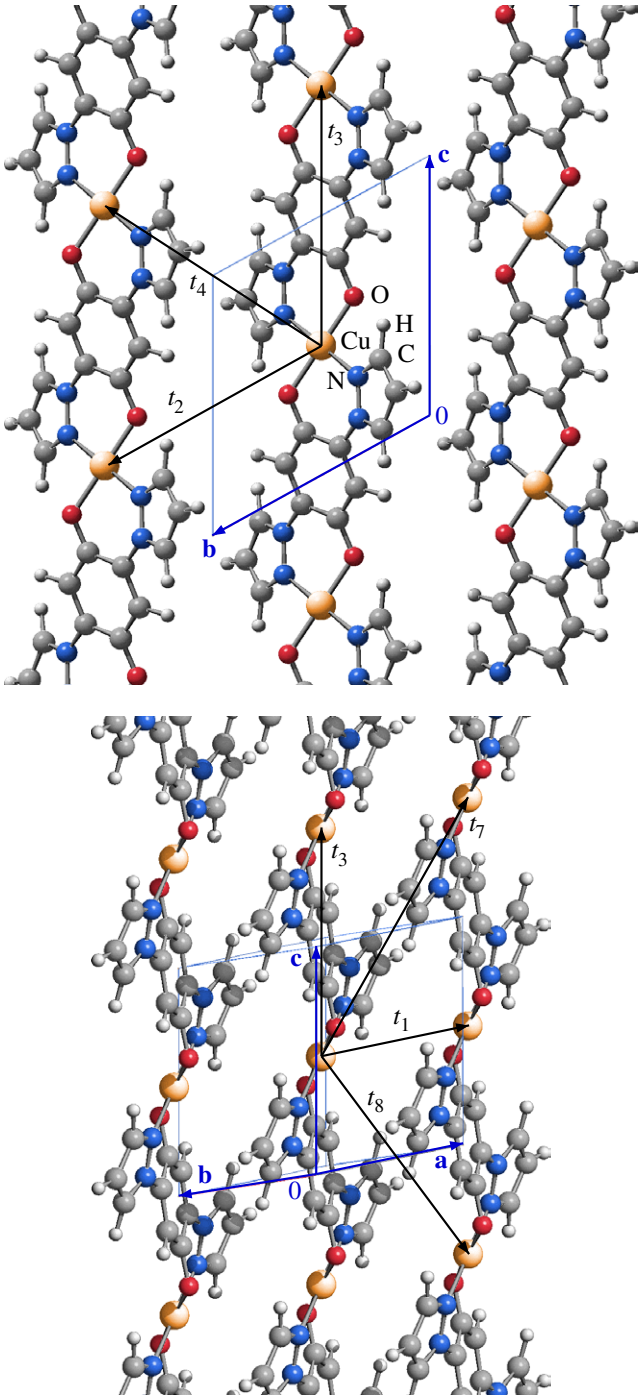

Figure 2. Crystal structure of the CuCCP polymer in two different orientations. The unit cell is shown in the figures (vectors **a, b** and **c**). Note the arrangements of the Cu chains along the c-direction. The various Cu–Cu interaction paths t_i have been also drawn where the index $i = 1, 2, 3, 7, 8$ denotes the ith nearest neighbour.

Table 2. Lattice parameters for the experimental crystal structure CuCCP and models Cu(II)-H_2O and Cu(II)-NH_3, optimized with force field methods.

Structure	a(Å)	b(Å)	c(Å)	α(°)	β(°)	γ(°)	V(Å^3)
CuCCP exp	5.172	7.959	8.230	118.221	91.520	100.148	291.47
Cu(II)–H_2O	5.234	11.249	8.072	117.611	68.822	127.155	330.43
Cu(II)–NH_3	5.459	11.597	8.349	118.423	68.840	130.883	350.49

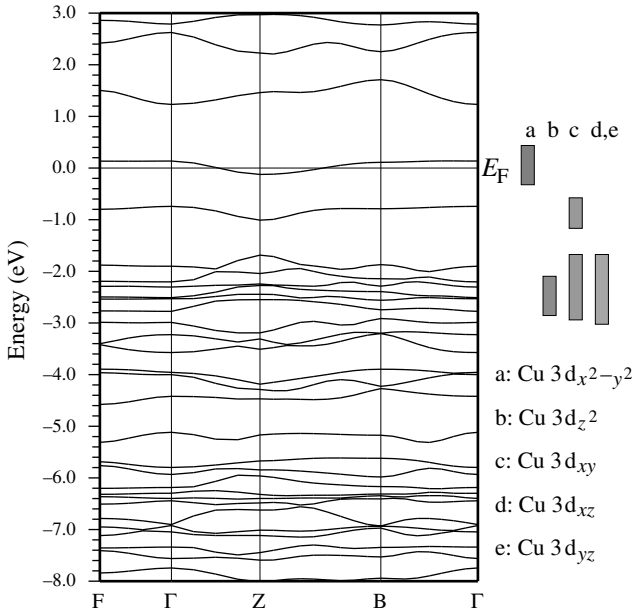

Figure 3. Band structure for the relaxed Cu(II) polymer CuCCP in the GGA approximation along the path [39] F(0, 1, 0)–Γ(0, 0, 0)–Z(0, 0, 1)–B(0.99, −0.13, 0)–Γ(0, 0, 0) in units of π/a, π/b, π/c. The bars indicate the dominant band character in the local coordinate frame of Cu (see text for explanation).

local coordinate frame of Cu which is defined with the local z-direction pointing from the Cu to out-of-plane N atom in the next layer and the y-direction pointing from the Cu to in-plane O atom. Cu is in a $3d^9$ configuration, with all d bands occupied except for the last band which is half-filled. GGA predicts a metallic behaviour for this system. As mentioned previously, inclusion of on-site electronic correlation within LDA + U opens a gap between a lower occupied Hubbard band and an upper unoccupied Hubbard band and the system is described as a Mott–Hubbard insulator. Since the O–Cu–N angle in the CuO_2N_2 plane is not exactly 90°, the various Cu d degrees of freedom defined with respect to the local coordinate frame mentioned above show slight admixtures. In particular, the Cu $d_{x^2-y^2}$ dominated band crossing the Fermi level has also small contributions from Cu d_{yz} degrees of freedom which arise from the distorted geometry.

From the dispersion of the Cu d band at the Fermi level, we confirm the one-dimensionality of the structure. The paths F–Γ and B–Γ which correspond to the inter-chain paths are almost

Table 3. Values for the Cu–Cu hopping integrals calculated with the NMTO downfolding method for the relaxed CuCCP, Cu(II)–NH_2 and Cu(II)–CN structures. The values are given in meV. The subscripts $i = 1, 2, 3, 7, 8, 12$ denote the ith nearest neighbours. See figure 2. Only the hopping integrals having values larger than or equal to one tenth of a meV have been shown.

Path	CuCCP	Cu(II)–NH_2	Cu(II)–CN
t_1	4	9	22
t_2	8	3	0
t_3	79	88	68
t_7	5	1	9
t_8	3	8	8
t_{12}	0	0	9

dispersionless and the intrachain Γ–Z–B path shows a cosine-like behaviour. A quantitative analysis of the various hopping integrals obtained with the downfolding procedure, by keeping only the Cu $d_{x^2-y^2}$ degrees of freedom active and integrating out all the rest within the NMTO framework, is given in the first column of table 3. The various interaction paths are as shown in figure 2. The largest hopping integral t_3 is along the chain (see figure 2), while all other hoppings are almost an order of magnitude smaller.

3.2.2. Cu(II)–NH_2 and Cu(II)–CN. In order to have a quantitative account of the structural changes that the polymer system undergoes under the various substitutions, we define the angle between the vector perpendicular to the CuO_2N_2 plane and the vector perpendicular to the benzene ring as the tilting angle ϑ. The substitution of H by NH_2 groups or CN groups in the benzene rings induces a tilting from $\vartheta = 34.9^\circ$ in CuCCP to $\vartheta = 37.3^\circ$ in Cu(II)–NH_2 and $\vartheta = 36.3^\circ$ in Cu(II)–CN.

In figures 4 (a) and (b), we present the FPLAPW orbital resolved DOS for the Cu(II)–NH_2 and the Cu(II)–CN within the GGA approximation. Shown is the contribution to the total DOS of Cu, O, N, C and the groups NH_2 and CN. While some changes in the detailed shape of the DOS for Cu, O, N and C between figures 4 (a) and (b) are observed, the most important effect is the different electronic nature of the NH_2 and CN groups. Figure 4 (c) shows the contribution of these groups at the Fermi surface. The CN group bands are deep down into the valence band while the NH_2 group has appreciable contribution near the Fermi level, which indicates its involvement in the effective interaction paths between copper atoms. We will see this more clearly in the plot of the NMTO-Wannier orbitals to be discussed later in this section.

In figure 5, we show a comparison of the band structure for the relaxed CuCCP, Cu(II)-NH_2 and the Cu(II)–CN polymers in the energy range $[-0.25\,\text{eV}, 0.25\,\text{eV}]$ where only the Cu $d_{x^2-y^2}$ dominated band is involved. Though the basic nature of the dispersion remains the same upon substitution, the details however do change. NH_2 seems to be the most effective substitution to increase the intrachain Cu–Cu interaction (the bandwidth widens along the Γ–Z–B path for the Cu(II)–NH_2 system). The CN substitution, on the other hand, reduces this interaction (note the bandwidth narrowing along the Γ–Z–B path for the Cu(II)–CN system). The substitution process also enhances certain interchain couplings. The almost dispersionless behaviour along F–Γ and B–Γ becomes more dispersive. Description of such fine and subtle changes needs some

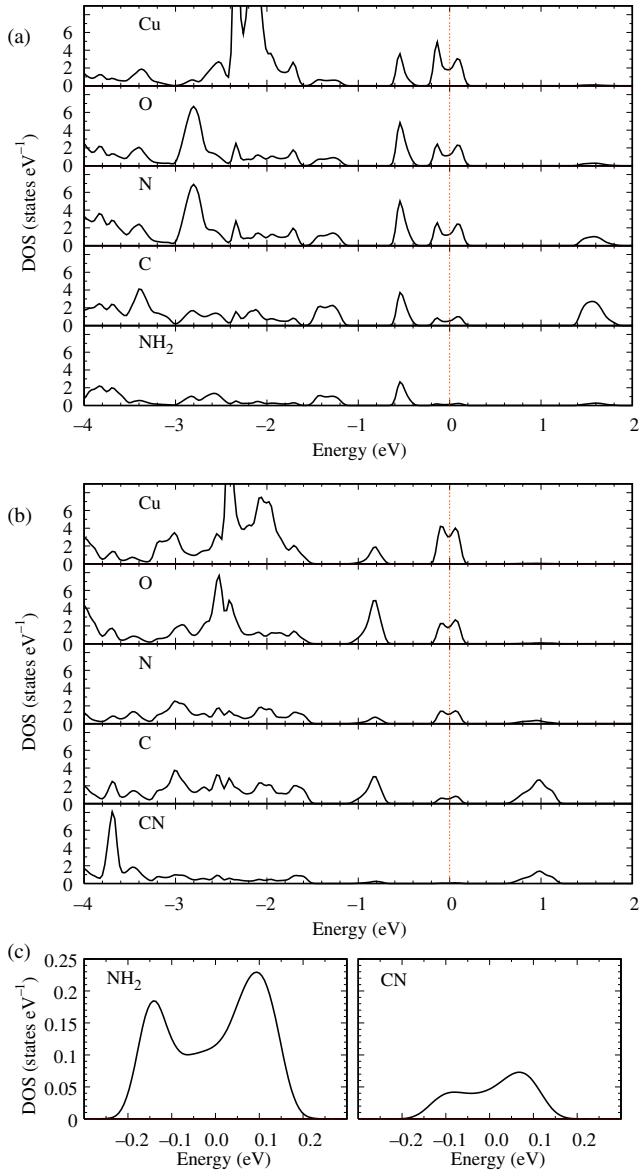

Figure 4. Orbital resolved DOS for (a) Cu(II)–NH_2 and (b) Cu(II)–CN. Panel (c) shows the comparison of the contribution of the NH_2 and CN groups to the DOS at E_F in a blown up scale.

quantitative measures which can be best described by the changes in effective Cu–Cu hoppings. This is shown in table 3, where the hopping integrals obtained by the NMTO downfolding method are shown. Note that the t_1 hopping for the Cu(II)–CN system along the crystallographic a-direction is enhanced by a factor of 4.5. Similarly, t_7 and t_8 hopping terms for the Cu(II)–CN system between neighbouring Cu chains in the b-direction (see figure 2) are almost 2–3 times larger compared to that of the CuCCP system. The long-ranged t_{12} hopping parameter between neighbouring chains along the a-axis also attains appreciable enhancement compared to a vanishingly small value for the CuCCP system. Similarly, t_1 and t_8 hoppings are enhanced for the NH_2 substitution by factors of ≈2–3. Among all the hoppings, only t_2 shows the exception of

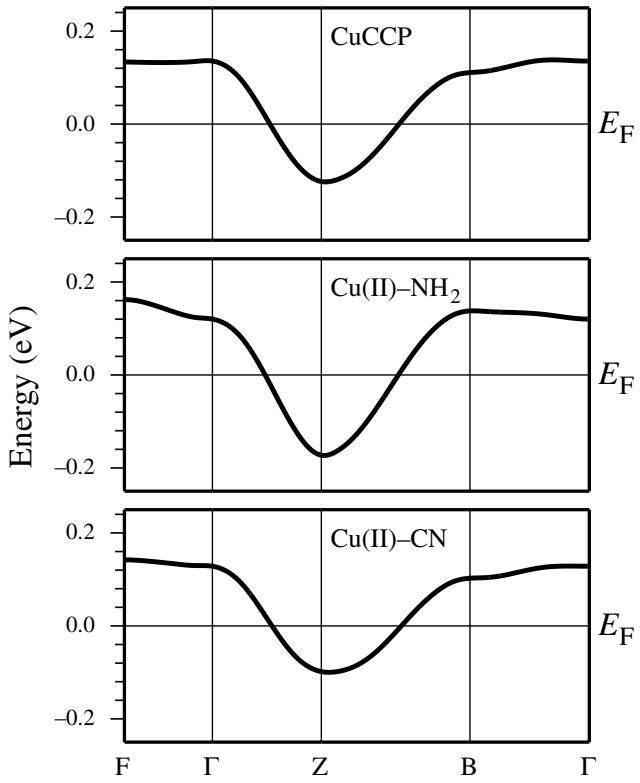

Figure 5. Comparison between the band structures for (from top to bottom) the relaxed CuCCP, Cu(II)–NH_2 and Cu(II)–CN respectively.

being systematically decreased upon substitution. The predominant hopping, t_3 is enhanced in the Cu(II)–NH_2 system and reduced in the Cu(II)–CN system as already predicted from bandwidth arguments.

A very helpful tool to understand the origin of these changes is the plot of effective Cu Wannier orbitals. In figure 6, we show the Wannier orbitals for the three Cu(II) systems presented so far. The plotted Wannier orbitals are obtained with the NMTO downfolding technique as introduced in subsection 2.2.

The effective Cu Wannier orbital has the expected Cu $d_{x^2-y^2}$ symmetry at the central Cu site while the tails sitting at other sites are shaped according to the symmetries of the various integrated out orbitals like the rest of the Cu d orbitals, O p, N p or C p. Note that the Cu d, O p and N p antibonding orbitals in the basic CuN_2O_2 square plaquette remain similar in all three cases but the effective orbital distribution in the benzene ring is markedly different. The changes are most prominent for the NH_2 substituted case with the tails attaining appreciable weight at the sites in the benzene ring. We also notice the occurrence of weight at the NH_2 assembly which is in accordance with the orbital resolved DOS study (see figure 4). This leads to an enhancement in both intra- and some interchain Cu–Cu interactions, caused by the larger overlap of the effective orbitals. The enhancement happens via two different routes: one is due to the different tilting of the benzene ring compared to the original compound and the other one is the opening of additional interaction paths via the NH_2 group which enhances the intrachain as well as interchain interactions t_1 and t_8 as can be seen in the quantitative estimates of the hopping interactions in table 3. In the case of the CN substitution, the opening of an additional

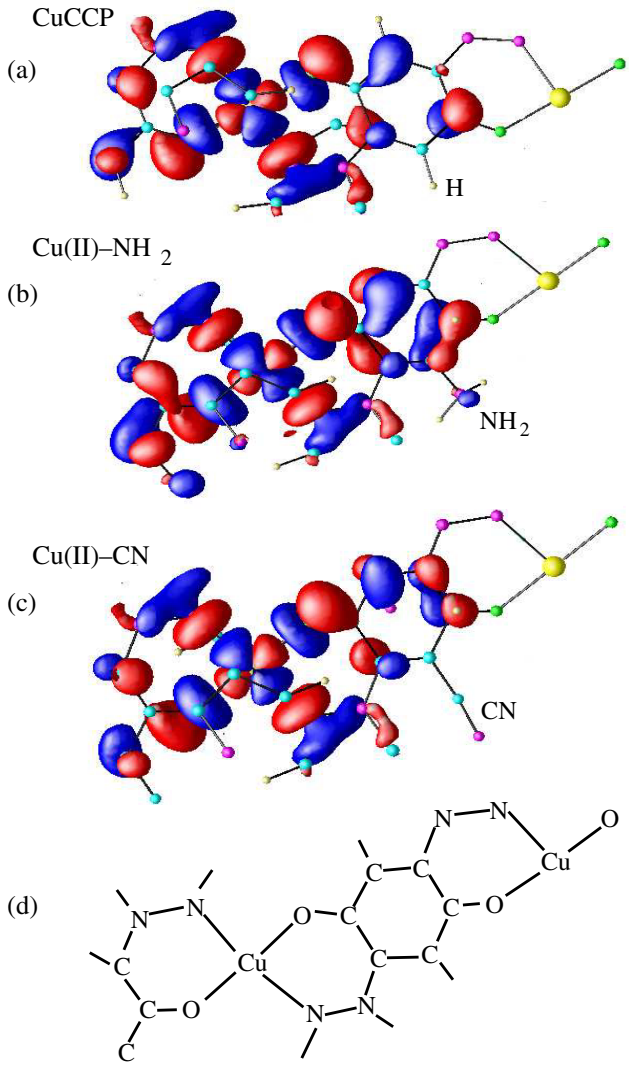

Figure 6. Cu Wannier functions for (a) the relaxed CuCCP polymer, (b) the Cu(II)–NH_2 polymer, and (c) the Cu(II)–CN polymer. (d) Indicates the atom positions common to (a)–(c). The N–C–C–C–H chain of atoms appearing above the Wannier function belongs to the next layer.

intrachain pathway is absent, which is reflected in the reduced intrachain (t_3) hopping interaction. However the mechanism via the tilting of the benzene ring is still operative which is seen in the enhancement of several interchain couplings, especially t_1.

Relating the magnetic coupling interaction J with the effective hopping interaction t via a relationship $J_{\mathrm{AFM}} \approx 4t^2/U_{\mathrm{eff}}$, as discussed in subsection 2.2, and choosing U_{eff} to be 5 eV[8], we obtain the nearest-neighbour coupling for the CuCCP system to be $J_{\mathrm{AFM}} \approx 58$ K which is somewhat larger than the experimental estimate [5] obtained by fitting susceptibility data to an effective nearest-neighbour Heisenberg model, but remains of the same order of magnitude.

[8] Note that this is a very rough U_{eff} estimate since we have here Cu surrounded by two O and two N atoms and the Cu–Cu path is via a complicated organic linker. Typical values of U_{eff} for Cu oxides are 4–6 eV.

Table 4. Values for the Cu–Cu hopping integrals calculated with the NMTO downfolding method for the relaxed CuCCP, Cu(II)-H_2O and Cu(II)-NH_3 structures. The values are given in meV. The subscripts $i = 1, 2, 3, 7, 8, 12$ denote the ith nearest neighbours. See figure 2.

Path	CuCCP	Cu(II)–H_2O	Cu(II)–NH_3
t_1	4	8	11
t_2	8	7	5
t_3	79	57	22
t_7	5	1	1
t_8	3	0	0
t_{12}	0	0	0

The J_{AFM} values estimated for Cu(II)–NH_2 and Cu(II)–CN systems are $J_{AFM} \approx 72$ K and $\approx$43 K respectively.

3.2.3. Cu(II)–H_2O and Cu(II)–NH_3. In our second set of modifications, we introduce two kinds of ligands, H_2O and NH_3 in the CuCCP system in the way presented in subsection 3.1. Our goal is to study the effect of H_2O and NH_3 satellites on the CuCCP structure as well as to search for possible routes to change the Cu coordination from planar to octahedral. As explained in subsection 3.1, in order to obtain realistic structures, the optimization with the force field method was done without keeping the original cell fixed, since that would force very short intermolecular distances between the H_2O (NH_3) moieties and the neighbouring chains. The force field optimized structures (see table 2) and subsequently relaxed with AIMD are characterized by Cu–O (O of the H_2O molecule) distances of $d_{CuO} = 2.17$ Å while the Cu–O and Cu–N in-plane distances are $d_{CuO} = 1.99$ Å and $d_{CuN} = 2.01$ Å, respectively. This corresponds to a distorted octahedron elongated along the Cu–H_2O direction. For the case of the NH_3 ligands the Cu–N (N of the NH_3 molecule) distances are $d_{CuN} = 2.14$ Å, while the Cu–O and Cu–N in-plane distances are $d_{CuO} = 2.02$ Å and $d_{CuN} = 2.03$ Å, also giving rise to an elongated octahedron along the Cu–NH_3 direction. The ligands close to the Cu(II) centre also induce a tilting of the benzene rings with respect to the CuO_2N_2 plane. From the initial angle of $\vartheta = 34.9^\circ$ in CuCCP the tilting due to the H_2O ligand is quite significant, leading to $\vartheta = 42.9^\circ$ in Cu(II)–H_2O. The NH_3 molecule, by contrast, leads to a lowering of this angle to $\vartheta = 31.8^\circ$ in Cu(II)–NH_3.

In order to quantify the effect of the H_2O and NH_3 ligands on the electronic properties of CuCCP, we show in table 4 the values of the Cu–Cu hopping integrals calculated with the NMTO downfolding method where the hopping parameters for the original CuCCP have been included for comparison. Note that the intrachain Cu–Cu coupling is reduced by a factor of 1.5–3.5 with the inclusion of both ligands. The reduction is especially significant with NH_3. The only Cu–Cu interchain path that is enhanced is t_1 which is between Cu in nearest-neighbour chains and has its origin in the hydrogen bonds between the H of the H_2O (NH_3) molecule and the O of the hydroquinone fragments in the chains. Therefore, apart from these hydrogen bonds, the introduction of ligands isolates the Cu ions considerably.

In the Wannier orbital plot in figures 7 and 8, we can see that the distorted octahedral environment of the Cu in the Cu(II)–H_2O and Cu(II)–NH_3 structures induces very little mixing of the Cu d_{z^2} orbital to the predominant $d_{x^2-y^2}$. Also note the little contribution of weight in the hydroquinone ring, in contrast to the previously discussed systems (see figure 6) which is a

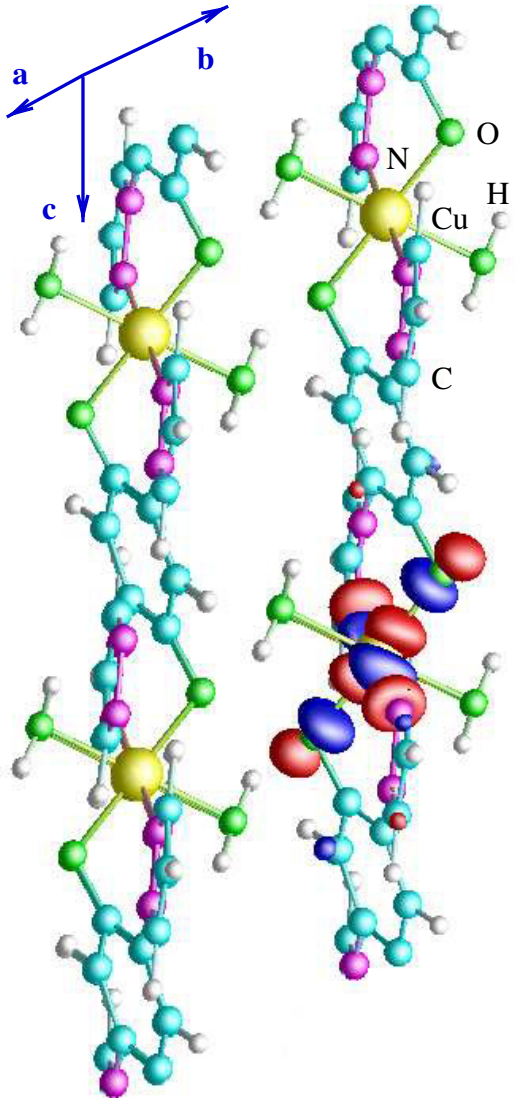

Figure 7. Cu Wannier functions for the Cu(II)–H_2O system.

manifestation of the isolated nature of Cu in these structures. The inclusion of the H_2O and NH_3 satellites, however, changes the Cu coordination only marginally from four in the direction of six, as opposed to our original motivation for the addition of H_2O and NH_3 ligands. Cu remains in the oxidation state of almost 2+ as observed in our calculations. While the GGA calculations give a metallic behaviour with a half-filled predominantly $d_{x^2-y^2}$ Cu band, inclusion of correlation effects with LDA + U drive the system to an insulating state. Therefore the system will remain an insulator.

4. Summary

In search of low-dimensional quantum spin systems with tunable properties, we have proposed and analysed within an *ab initio* framework and using a combination of different computational methods various chemical modifications to the Cu-based polymeric coordination compound

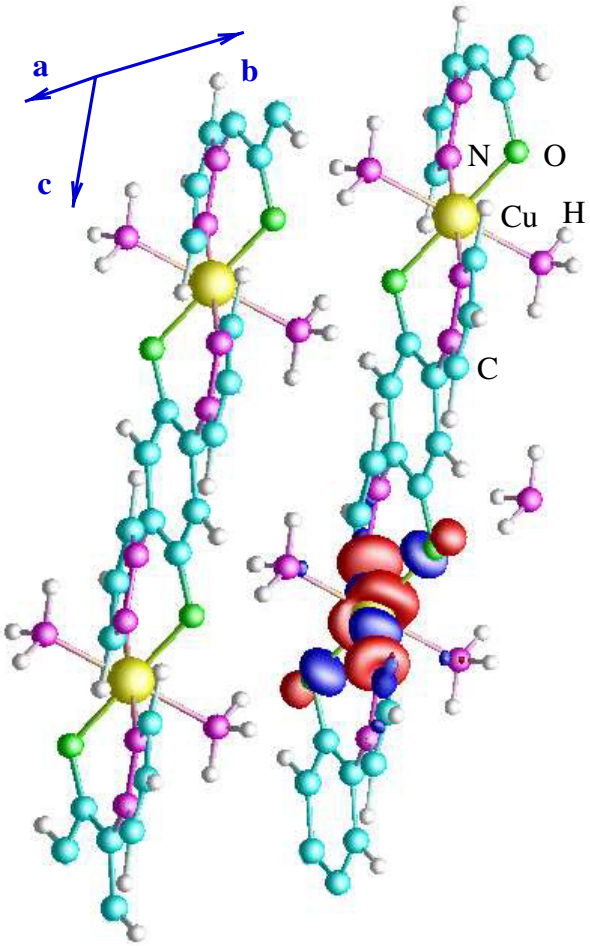

Figure 8. Cu Wannier functions for the Cu(II)–NH_3 system.

CuCCP. Our goal has been to tune in a controlled way the magnetic interactions between Cu centres and to test the efficiency and feasibility of the combination of methods proposed here. We pursued two ways of modifying the original CuCCP structure; by changing the substitution pattern in the linker (hydroquinone) and by adding ligands to the system. Following the first scheme, we considered two possible H substitutions in the hydroquinone; an electron donating group (NH_2) and an electron withdrawing group (CN). For the second scheme, we considered structures with H_2O and NH_3 ligands. Out of our study, we conclude that the NH_2 substitution in the hydroquinone is the most effective in order to enhance the intrachain Cu–Cu interaction in CuCCP while the CN substitution induces and enhances the interchain interactions in the system which were either absent or very weak in the original CuCCP compound. In contrast, the inclusion of H_2O or NH_3 ligands has the effect of isolating the Cu ions.

The effects observed in this study are small, mainly due to the fact that the coupling constants in these metalorganic materials are weak. On the other hand, these systems are, due to the smallness of the coupling constants, of special interest since application of moderate magnetic fields or pressure can drive the system to a phase transition. These systems can be described as Mott–Hubbard insulators and possibly under application of pressure a metal–insulator transition could be induced. This will form the basis of future studies.

Table A1. Fractional atomic coordinates of non-equivalent atoms in the CuCCP relaxed structure. For the lattice parameters, see table 2.

Atom	*x*	*y*	*z*
Cu	0.5000	0.5000	0.5000
O2	0.4581	0.3495	0.6187
C3	0.4745	0.4243	0.7998
C4	0.6696	0.5869	0.9293
C5	0.0331	0.7729	0.6797
C6	0.2206	0.8455	0.8363
C7	0.1024	0.7795	0.9497
C8	0.6971	0.6615	0.1203
N9	0.8576	0.6739	0.8610
N10	0.8109	0.6692	0.6956
H11	0.1732	0.7923	0.0815
H12	0.4193	0.9317	0.8607
H13	0.0456	0.7875	0.5549
H14	0.8471	0.7919	0.2121

Finally, we believe that the combination of methods presented in the manuscript is efficient for studying the properties of complex systems *per se*, and that the computer-designing procedure that we have employed in the present study provides a plausible route for manipulating properties related to low-dimensional quantum spin systems in general.

Acknowledgments

We thank M Wagner for useful discussions and T Kretz for providing the information about aminophenol and *o*-cyanophenol. This study was financially supported by the Deutsche Forschungsgemeinschaft (DFG) through the Forschergruppe FOR 412 and HOJ gratefully acknowledges support from the DFG through the Emmy Noether Program. We gratefully acknowledge support by the Frankfurt Center for Scientific Computing. TSD and BR acknowledge collaboration with the MPG-India partnergroup program.

Appendix

We present here the AIMD relaxed structural data of the various Cu(II) polymers. Other than CuCCP, the rest are computer designed.

In table A1, we show the fractional atomic positions of the CuCCP polymer obtained after the relaxation of the system. The resulting distances between the atoms after the optimization are closer to the standard values found in [40] but differ from the values for the distances in the experimental compound [4].

In table A2, we present the relative atomic positions obtained after relaxation for Cu(II)–CN. The cell parameters were fixed during relaxation, and the only change observed was the tilting of the hydroquinone ring as a consequence of the upward movement of the pyrazolyl rings.

In table A3 we show the same, but for Cu(II)–NH_3.

The structural data for the Cu(II)–NH_2 and Cu(II)–H_2O systems have already been presented in [3].

Table A2. Fractional atomic positions of non-equivalent atoms in Cu(II)–CN obtained with the PAW method. For the lattice parameters, see table 2 (same as CuCCP).

Atom	x	y	z
Cu	0.5000	0.5000	0.5000
O2	0.4559	0.3460	0.6195
C3	0.4823	0.4252	0.7998
C4	0.6795	0.5881	0.9253
C5	0.0384	0.7593	0.6620
C6	0.2349	0.8314	0.8139
C7	0.1239	0.7694	0.9310
C8	0.6944	0.6601	0.1182
C9	0.1030	0.1811	0.7598
N10	0.8687	0.6739	0.8553
N11	0.8152	0.6676	0.6880
N12	0.9162	0.0575	0.6788
H13	0.2104	0.7793	0.0570
H14	0.4353	0.9135	0.8323
H15	0.0493	0.7681	0.5346

Table A3. Fractional atomic positions of non-equivalent atoms in Cu(II)–NH_3 obtained with the PAW method. For the lattice parameters, see table 2.

Atom	x	y	z
Cu	0.5000	0.5000	0.5000
O2	0.4679	0.3798	0.6285
C3	0.4786	0.4444	0.8064
C4	0.6761	0.6148	0.9103
C5	0.0881	0.8540	0.6283
C6	0.2867	0.9709	0.7753
C7	0.1520	0.8949	0.9023
C8	0.6932	0.6630	0.0956
N9	0.8861	0.7410	0.8310
N10	0.8489	0.7159	0.6631
H11	0.2228	0.9402	0.0374
H12	0.4977	0.0958	0.7892
H13	0.0972	0.8601	0.4997
H14	0.8313	0.7917	0.1793
N15	0.8587	0.4701	0.3123
H16	0.7612	0.3507	0.2812
H17	0.0789	0.5407	0.3673
H18	0.9088	0.4872	0.1907

References

[1] Kahn O and Martinez C J 1998 *Science* **279** 44
[2] Postnikov A V, Kortus J and Pederson M R 2004 *Psi-k Newsletter* no. 61, p 127
[3] Jeschke H O, Salguero L A, Valentí R, Buchsbaum C, Schmidt M U and Wagner M 2007 *C. R. Chim.* at press doi: 10.1016/j.crci.2006.06.007
[4] Dinnebier R, Lerner H W, Ding L, Shankland K, David W I F, Stephens P W and Wagner M 2002 *Z. Anorg. Allg. Chem.* **628** 310
[5] Wolf B *et al* 2004 *Phys. Rev.* B **69** 092403
[6] Singh R R P, Fleury P A, Lyons K B and Sulewski P E 1989 *Phys. Rev. Lett.* **62** 2736
[7] Schmidt M U and Englert U 1996 *J. Chem. Soc. Dalton Trans.* **1996** 2077
[8] Verwer P and Leusen F J J 1998 *Rev. Comput. Chem.* **12** 327
[9] Mooij W T M, van Eijck B P, Price S L, Verwer P and Kroon J 1998 *J. Comput. Chem.* **19** 459
[10] Lommerse J P M *et al* 2000 *Acta Cryst.* B **56** 697
[11] Motherwell W D S *et al* 2002 *Acta Cryst.* B **58** 647
[12] Day G M *et al* 2005 *Acta Cryst.* B **61** 511
[13] Schön J C and Jansen M 2001 *Z. Krist.* **216** 307
[14] Schön J C and Jansen M 2001 *Z. Krist.* **216** 361
[15] van Eijck B P, Mooij W T M and Kroon J 2001 *J. Comput. Chem.* **22** 805
[16] Mooij W T M, van Duijnefeldt F B, van de Rijdt J G C M and van Eijck B P 1999 *J. Phys. Chem.* A **103** 9872
[17] Mooij W T M, van Eijck B P and Kroon J 1999 *J. Phys. Chem.* A **103** 9883
[18] 2005 *Cambridge Structural Database* (Cambridge, England: Cambridge Crystallographic Data Centre)
[19] Car R and Parrinello M 1985 *Phys. Rev.* B **55** 2471
[20] 2003 *Cerius2, Version 4.9* (Cambridge, UK: Accelrys)
[21] Mayo S L, Olafson B D and Goddard W A III 1990 *J. Phys. Chem.* **94** 8897
[22] Gasteiger J and Marsili M 1980 *Tetrahedron* **36** 3219
[23] Blöchl P E 1994 *Phys. Rev.* B **50** 17953
[24] Blaha P, Schwarz K, Madsen G K H, Kvasnicka D and Luitz J 2001 *WIEN2K, An Augmented Plane Wave + Local Orbitals Program for Calculating Crystal Properties* ed K Schwarz (Wien, Austria: Techn. University) ISBN 3-9501031-1-2
[25] Perdew J P, Burke S and Ernzerhof M 1996 *Phys. Rev. Lett.* **77** 3865
[26] Anisimov V I, Zaanen J and Andersen O K 1991 *Phys. Rev.* B **44** 943
[27] Petukhov A G, Mazin I I, Chioncel L and Lichtenstein A I 2003 *Phys. Rev.* B **67** 153106
[28] Pavarini E, Yamasaki A, Nuss J and Andersen O K 2005 *New J. Phys.* **7** 188
[29] Andersen O K, Saha-Dasgupta T and Ezhov S 2003 *Bull. Mater. Sci.* **26** 19
[30] Andersen O K and Saha-Dasgupta T 2000 *Phys. Rev.* B **62** R16219
[31] Andersen O K, Saha-Dasgupta T, Ezhov S, Tsetseris L, Jepsen O, Tank R W, Arcangeli C and Krier G 2001 *Psi-k Newsletter* no. 45, pp 86–119
[32] Pavarini E, Dasgupta I, Saha-Dasgupta T, Jepsen O and Andersen O K 2001 *Phys. Rev. Lett.* **87** 047003
[33] Sarma D D, Mahadevan P, Saha-Dasgupta T, Ray S and Kumar A 2000 *Phys. Rev. Lett.* **85** 2549
[34] Valentí R, Saha-Dasgupta T, Alvarez J V, Pozgajcic K and Gros C 2001 *Phys. Rev. Lett.* **86** 5381
[35] Valentí R and Saha-Dasgupta T 2002 *Phys. Rev.* B **65** 144445
[36] Valentí R, Saha-Dasgupta T and Gros C 2002 *Phys. Rev.* B **66** 054426
[37] Saha-Dasgupta T and Valentí R 2002 *Europhys. Lett.* **60** 309
[38] Valentí R, Saha-Dasgupta T, Gros C and Rosner H 2003 *Phys. Rev.* B **67** 245110
[39] Bradley C J and Cracknell A P 1972 *The Mathematical Theory of Symmetry in Solids: Representation Theory for Point Groups and Space Groups* (Oxford: Oxford University Press)
[40] Allen F H, Kennard O, Watson D G, Brammer L, Orpen A G and Taylor R 1987 *J. Chem. Soc. Perkin Trans.* II **1987** 1